Supramolecular Ru and/or Os Complexes of Tris(bipyridine) Bridging Ligands. Syntheses, Absorption Spectra, Luminescence Properties, Electrochemical Behavior, Intercomponent Energy, and Electron Transfer

Peter Belser,*[1a] Alex von Zelewsky,[1a] Michael Frank,[1b] Christian Seel,[1b] Fritz Vögtle,*[1b] Luisa De Cola,*[1c] Francesco Barigelletti,[1d] and Vincenzo Balzani*[1c]

Contribution from the Institut für Anorganische Chemie, Universität Freiburg, Freiburg, Switzerland, Institut für Organische Chemie und Biochemie, Universität Bonn, Bonn, Germany, and Dipartimento di Chimica "G. Ciamician" dell'Università and Istituto FRAE-CNR, Bologna, Italy

Received July 20, 1992

Abstract: The tris(bipyridine) tripod ligands 1,3,5-tris[4-(((2,2′-bipyridyl-5-yl)carbonyl)benzylamino)methyl]benzene (**1**), 1,3,5-tris[4-(((2,2′-bipyridyl-5-ylcarbonyl)benzylamino)methyl)phenyl]benzene (**2**), and 1,3,5-tris[4-((((2,2′-bipyridyl-5-ylcarbonyl)benzylamino)methyl)phenylyl)phenyl]benzene (**3**) have been synthesized and their complexes **1**$[Ru(bpy)_2]^{2+}$, **1**$[Ru(bpy)_2]_2^{4+}$, **1**$[Ru(bpy)_2]_3^{6+}$, **1**$[Os(bpy)_2]_3^{6+}$, **1**$[Ru(bpy)_2]_2[Os(bpy)_2]^{6+}$, **2**$[Ru(bpy)_2]_3^{6+}$, **2**$[Os(bpy)_2]_3^{6+}$, **2**$[Ru(bpy)_2]_2[Os(bpy)_2]^{6+}$, and **3**$[Ru(bpy)_2]_3^{6+}$ have been prepared. All the complexes display very intense, ligand centered absorption bands in the UV region and moderately intense metal-to-ligand charge-transfer bands in the visible. Electrochemical oxidation of each Ru(II) or Os(II) metal center occurs always at the same potential (+1.30 V for Ru(II), +0.87 V for Os(II)), regardless of tripod ligand and number and type of metal-based units that are present in the supramolecular structure. The five homometallic Ru(II) species exhibit the same luminescence properties, and this is also the case for the two homometallic Os(II) species. The luminescence data obtained for the two mixed-metal species show that electronic energy transfer takes place from the Ru-based to the Os-based components. The efficiency of energy transfer decreases in going from **1**$[Ru(bpy)_2]_2[Os(bpy)_2]^{6+}$ to **2**$[Ru(bpy)_2]_2[Os(bpy)_2]^{6+}$, i.e., as the size of the spacer which links the three arms of the bridging ligand increases. Oxidation of **1**$[Ru(bpy)_2]_3^{6+}$, **2**$[Ru(bpy)_2]_3^{6+}$, **1**$[Os(bpy)_2]_3^{6+}$, and **2**$[Os(bpy)_2]_3^{6+}$ by Ce(IV) leads to mixed-valence species where the oxidized metal-based units quench the luminescent excited state of the units that are not oxidized. The quenching efficiency decreases as the size of the spacer increases. The mechanisms of the quenching processes are discussed. The results obtained indicate that at least in the case of the trinuclear species of **2**, there are conformers in which the quenching can take place very rapidly and conformers where it does not take place at all.

Introduction

Ru(II) and Os(II) polypyridine complexes have been extensively investigated in the past two decades because of their outstanding luminescence[2] and electrochemical[2,3] properties. In the last few years it has been shown that such complexes can be used as building blocks to synthesize polynuclear complexes which behave as supramolecular species.[4-7] Photoinduced energy and electron-transfer processes in supramolecular species[5,6,8] are currently the object of much interest in view of the design of photochemical molecular devices[5] that can perform useful functions in several fields, such as information recording[9] and conversion of light into chemical energy.[10]

In an attempt to elucidate the role played by various factors in determining the occurrence of photoinduced energy and electron-transfer processes in polymetallic complexes, we have designed and synthesized the tris(bipyridine) ligands **1**, **2**, and **3** (Figure 1) which can coordinate three (equivalent or different) metal-containing building blocks. **2** and **3** differ from **1** only for the presence of additional phenylene groups in each arm of the spacer S which bridges the three coordinating bpy-type sites. Coordination of $Ru(bpy)_2^{2+}$ and/or $Os(bpy)_2^{2+}$ units to such sites yields supramolecular species which contain three $M(bpy)_3^{2+}$-type complexes (M = Ru or Os) linked by a spacer (Figure 2). On the basis of previous investigations on mononuclear[2] and

(1) (a) University of Fribourg. (b) University of Bonn. (c) University of Bologna. (d) FRAE-CNR, Bologna.

(2) (a) Juris, A.; Balzani, V.; Barigelletti, F.; Campagna, S.; Belser, P.; von Zelewsky, A. *Coord. Chem. Rev.* **1988**, *84*, 85. (b) Meyer, T. J. *Pure Appl. Chem.* **1986**, *58*, 1193, and references therein. (c) Kalyanasundaram, K. *Photochemistry of Polypyridine and Porphyrin Complexes*; Academic Press: London, England, 1992.

(3) (a) Vlcek, A. A. *Coord. Chem. Rev.* **1982**, *43*, 39. (b) Lever, A. B. P. *Inorg. Chem.* **1990**, *29*, 1271.

(4) For reviews, see refs 5 and 6; for some recent papers, see ref 7.

(5) Balzani, V.; Scandola, F. *Supramolecular Photochemistry*; Horwood: Chichester, U.K., 1991.

(6) Scandola, F.; Indelli, M. T.; Chiorboli, C.; Bignozzi, C. A. *Top. Curr. Chem.* **1990**, *158*, 73.

(7) (a) Ryu, C. K.; Schmehl, R. H. *J. Phys. Chem.* **1989**, *93*, 7961. (b) Furue, M.; Yoshidzumi, T.; Kinoshita, S.; Kushida, T.; Nozakura, S.; Kamachi, M. *Bull. Chem. Soc. Jpn.* **1991**, *64*, 1632. (c) Strouse, G. F.; Worl, L. A.; Younathan, J. N.; Meyer, T. J. *J. Am. Chem. Soc.* **1989**, *111*, 9101. (d) Worl, L. A.; Strouse, G. F.; Younathan, J. N.; Baxter, S. M.; Meyer, T. J. *J. Am. Chem. Soc.* **1990**, *112*, 7571. (e) De Cola, L.; Barigelletti, F.; Balzani, V.; Hage, R.; Haasnoot, J. G.; Reedijk, J.; Vos, J. G. *Chem. Phys. Lett.* **1991**, *178*, 491. (f) Jones, W. E., Jr.; Baxter, S. M.; Mecklemburg, S. L.; Erickson, B. W.; Peek, B. M.; Meyer, T. J. In *Supramolecular Chemistry*; Balzani, V., De Cola, L., Eds.; Kluwer: Dordrecht, 1992; p 249. (g) de Wolf, J. M.; Hage, R.; Haasnoot, J. G.; Reedijk, J. *New J. Chem.* **1991**, *15*, 501. (h) Ryu, C. K.; Wang, R.; Schmehl, R. H.; Ferrere, S.; Ludwikow, M.; Merkert, J. W.; Headford, C. E. L.; Elliot, C. M. *J. Am. Chem. Soc.* **1992**, *114*, 430. (i) Bignozzi, C. A.; Bortolini, O.; Chiorboli, C.; Indelli, M. T.; Rampi, M. A.; Scandola, F. *Inorg. Chem.* **1992**, *31*, 172. (j) Denti, G.; Campagna, S.; Serroni, S.; Ciano, M.; Balzani, V. *J. Am. Chem. Soc.* **1992**, *114*, 2944.

(8) (a) Connolly, J. S.; Bolton, J. R. In *Photoinduced Electron Transfer*; Fox, M. A., Chanon, M., Eds.; Part D; Elsevier: New York, USA, 1988; p 303. (b) Wasielewski, M. R. In *Photoinduced Electron Transfer*; Fox, M. A., Chanon, M., Eds.; Part D; Elsevier: New York, USA, 1988; p 161. (c) Closs, G. L.; Miller, J. R. *Science* **1988**, *240*, 440. (d) Gust, D.; Moore, T. A. *Science* **1989**, *244*, 35. (e) Gust, D.; Moore, T. A. *Top. Curr. Chem.* **1991**, *159*, 103. (f) Vögtle, F. *Supramolecular Chemistry*; Wiley: Chichester, U.K., 1991. (g) *Supramolecular Chemistry*; Balzani, V., De Cola, L., Eds.; Kluwer: Dordrecht, The Netherlands, 1992.

(9) See, e.g.: Hopfield, J. J.; Onuchic, J. N.; Beratan, D. N. *J. Phys. Chem.* **1989**, *93*, 6350.

(10) See, e.g.: O'Regan, B.; Graetzel, M. *Nature* **1991**, *3531*, 737.

0002-7863/93/1515-4076$04.00/0

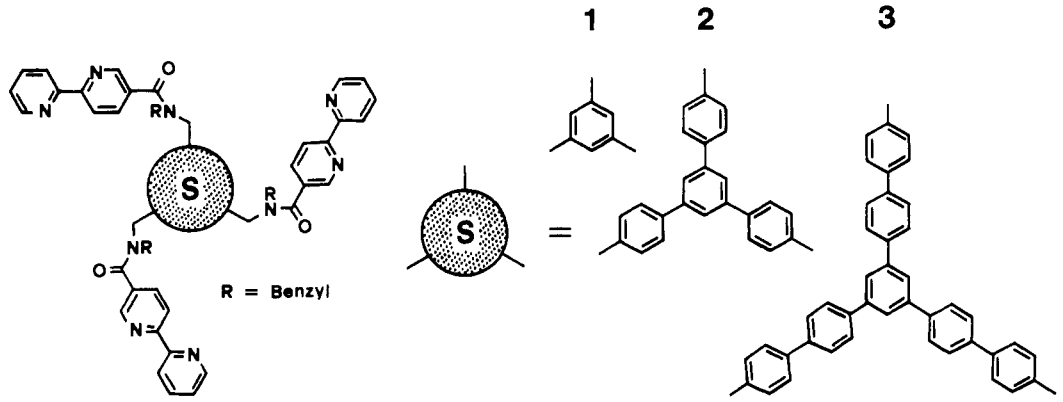

Figure 1. Structural formulae of the bridging ligands **1**, **2**, and **3**.

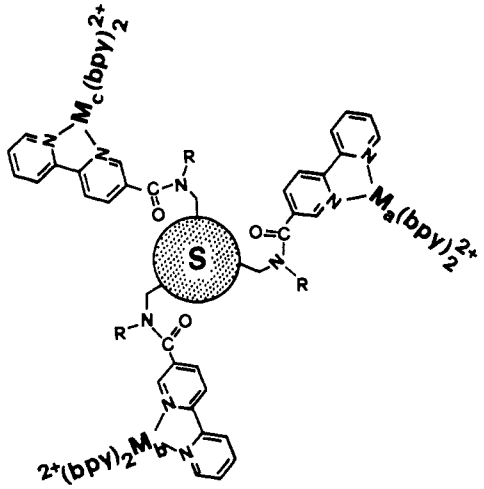

Figure 2. Structure of the trimetallic complexes. For the spacer S, see Figure 1.

oligonuclear[5,6] Ru(II) and Os(II) polypyridine complexes, it can be expected that the supramolecular species schematized in Figure 2 exhibit several interesting properties: (i) they should show intense absorption bands in the UV and visible spectral regions; (ii) they should display luminescence both in rigid matrix at 77 K and in fluid solution at room temperature; (iii) they should undergo reversible mono- and multielectron redox processes; (iv) energy transfer from the Ru-based to the Os-based units should take place in the Ru(II)–Os(II) mixed-metal species; and (v) photoinduced energy and/or electron-transfer processes should occur when the metal ions exhibit different oxidation states. Furthermore, it should be possible to study the interaction between excited chromophoric units upon laser excitation.

In this paper we describe the following: (a) the syntheses of the ligands **1**, **2**, and **3** and of their Ru(II) and Os(II) complexes; (b) the absorption spectra, luminescence properties, and electrochemical behavior of the following complexes (hereafter indicated by the abbreviations given in bold in parentheses, see also Table I), **1**$[Ru(bpy)_2]^{2+}$ (**1·Ru**), **1**$[Ru(bpy)_2]_2^{4+}$ (**1·Ru$_2$**), **1**$[Ru(bpy)_2]_3^{6+}$ (**1·Ru$_3$**), **1**$[Os(bpy)_2]_3^{6+}$ (**1·Os$_3$**), **1**$[Ru(bpy)_2]_2[Os(bpy)_2]^{6+}$ (**1·Ru$_2$Os**), **2**$[Ru(bpy)_2]_3^{6+}$ (**2·Ru$_3$**), **2**$[Os(bpy)_2]_3^{6+}$ (**2·Os$_3$**), **2**$[Ru(bpy)_2]_2[Os(bpy)_2]^{6+}$ (**2·Ru$_2$Os**), and **3**$[Ru(bpy)_2]_3^{6+}$ (**3·Ru$_3$**); (c) the intercomponent energy transfer in the **1·Ru$_2$Os** and **2·Ru$_2$Os** species; and (d) the changes observed in the absorption and luminescence spectra on addition of an oxidant to solutions of **1·Ru$_3$**, **2·Ru$_3$**, **1·Os$_3$**, and **2·Os$_3$** (i.e., in their mixed valence forms). Preliminary results on some of these species have already been reported.[11]

Experimental Section

Commercial 2-acetylpyridine, *N*,*N*-dimethylacetamide, triethylamine, 2,2′-bipyridine, $RuCl_3 \cdot 3H_2O$, and $(NH_4)_2OsCl_6$ were used as received.

Table I. Composition of the Complexes Studied

ligand[a]	metal ions[b] M_a	M_b	M_c	complex[c]
1	Ru^{2+}			**1.Ru**
1	Ru^{2+}	Ru^{2+}		**1.Ru$_2$**
1	Ru^{2+}	Ru^{2+}	Ru^{2+}	**1.Ru$_3$**
1	Os^{2+}	Os^{2+}	Os^{2+}	**1.Os$_3$**
1	Ru^{2+}	Ru^{2+}	Os^{2+}	**1.Ru$_2$Os**
2	Ru^{2+}	Ru^{2+}	Ru^{2+}	**2.Ru$_3$**
2	Os^{2+}	Os^{2+}	Os^{2+}	**2.Os$_3$**
2	Ru^{2+}	Ru^{2+}	Os^{2+}	**2.Ru$_2$Os**
3	Ru^{2+}	Ru^{2+}	Ru^{2+}	**3.Ru$_3$**

[a] See Figure 1. [b] See Figure 2. [c] Abbreviation used.

$Ru(bpy)_2Cl_2 \cdot 2H_2O$ and $Os(bpy)_2Cl_2$ were prepared according to literature procedures.[12,13] The solvents and reactants used were of the highest purity commercially available and were used as received.

Equipment and Methods. ^1H NMR spectra were recorded on a Gemini 300 Varian broadband spectrometer by using the proton impurities of the deuterated solvents as reference. The fast atomic bombardment mass spectral data (FAB) were obtained on a VG 7070 E spectrometer in a 3-nitrobenzyl alcohol matrix. Xe atoms were used for the bombardment (8 kV). Electron spray measurements were performed with a Finnigan TSQ 700 mass spectrometer with acetonitrile as solvent. Electrochemical measurements were carried out at room temperature (~25 °C) by using a Metrohm E/506 Polarecord, a Metrohm E/612 VA scanner, and a Hewlett-Packard 7044 x-y recorder. Cyclic voltammograms were obtained in acetonitrile solution by using a microcell equipped with a stationary platinum disk electrode, a platinum disk counter electrode, and a SCE reference electrode with tetrabutylammonium hexafluorophosphate as supporting electrolyte. In all cases $[Ru(bpy)_3](PF_6)_2$ was used as a standard, taking its oxidation potential equal to +1260 mV vs SCE.[14,15] The electrochemical window examined was between +2.0 and −2.0 V. Scanning speed was 200 mV s^{-1}. All the reported values are vs SCE. Half-wave potentials were calculated as an average of the cathodic and anodic peaks.

Luminescence experiments were performed in acetonitrile at room temperature and in a 4:5 v/v propionitrile–butyronitrile mixture at 77 K. The absorption spectra, emission spectra, luminescence decays, and electrochemical potentials were obtained as previously described.[16] Absorption spectra in the near infrared region were performed with a Perkin-Elmer lambda 9 UV–vis/NIR spectrophotometer. Interference

(11) (a) De Cola, L.; Barigelletti, F.; Balzani, V.; Belser, P.; von Zelewsky, A.; Seel, C.; Frank, M.; Vögtle, F. *Coord. Chem. Rev.* **1991**, *111*, 255. (b) De Cola, L.; Barigelletti, F.; Balzani, V.; Belser, P.; von Zelewsky, A.; Frank, M.; Seel, C.; Vögtle, F. In *Supramolecular Chemistry*; Balzani, V., De Cola, L., Eds.; Dordrecht: Kluwer, The Netherlands, 1992; p 157.

(12) Sullivan, B. P.; Salmon, D. J.; Meyer, T. J. *Inorg. Chem.* **1978**, *17*, 3334.

(13) Lay, P. A.; Sargeson, A. M.; Taube, H.; Chou, M. H.; Creutz, C. *Inorg. Synth.* **1986**, *24*, 294.

(14) Juris, A.; Balzani, V.; Belser, P.; von Zelewsky, A. *Helv. Chim. Acta* **1981**, *64*, 2175.

(15) Sutin, N.; Creutz, C. *Adv. Chem. Ser.* **1978**, *168*, 1. Lin, C. T.; Boettcher, W. J.; Chou, M.; Creutz, C.; Sutin, N. *J. Am. Chem. Soc.* **1976**, *98*, 6536.

(16) De Cola, L.; Belser, P.; Ebmeyer, F.; Barigelletti, F.; Vögtle, F.; von Zelewsky, A.; Balzani, V. *Inorg. Chem.* **1990**, *29*, 495.

Scheme I

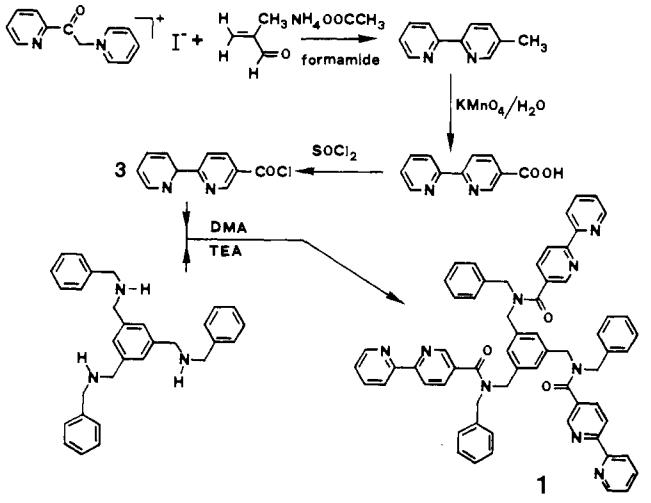

Scheme II

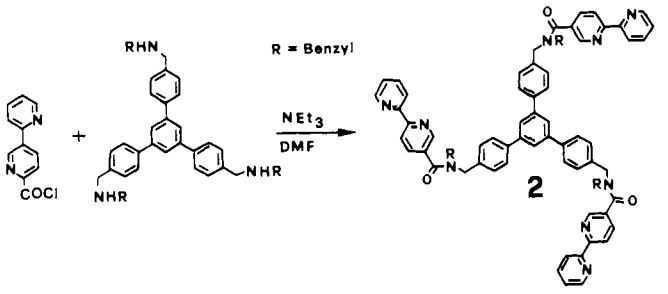

Scheme III

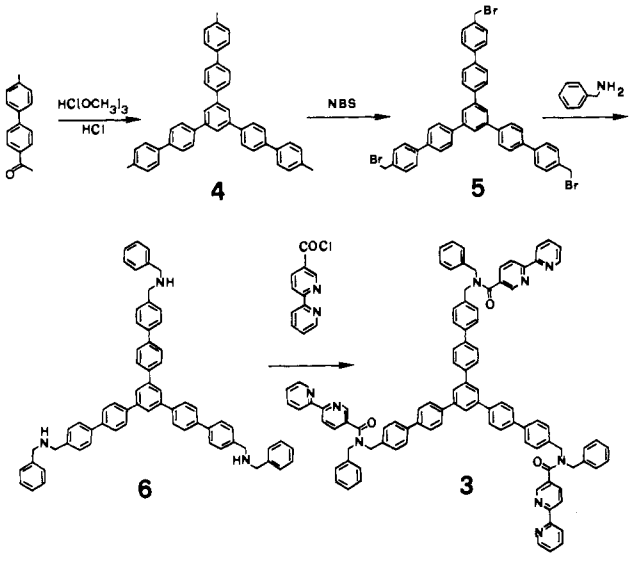

filters, cut-off filters, or monochromators were used to select appropriate spectral regions for lifetime measurements. Estimated errors: luminescence intensity, ±10%; excited state lifetime, ±8%.

Preparation of the Ligands. The ligand **1** was synthesized in a four step reaction illustrated in Scheme I. The pyridinium salt[17] of 2-acetylpyridine was transformed to 5-methyl-2,2′-bipyridine via the Kröhnke reaction.[18] The methyl group was then changed into a carboxylic group by oxidation with potassium permanganate.[19] The 2,2′-bipyridine-5-carboxylic acid was boiled in thionyl chloride to obtain the corresponding acid chloride. The condensation of three molecules of 2,2′-bipyridine-5-carboxylic chloride with one molecule of 1,3,5-tris[*N*-(benzylamino)-methyl]benzene[20] (spacer) gave the ligand **1**. In the last step of this synthesis, 2.5 g (5.74 mmol) of the spacer dissolved in 37 mL of *N*,*N*-dimethylacetamide (DMA) and 3.76 g (17.21 mmol) of 2,2′-bipyridine-5-carboxylic chloride dissolved in 84 mL of DMA were mixed together. Nine milliliters of triethylamine were then added, and the mixture was heated up to 120 °C and cooled down to room temperature. The solution was stirred overnight at room temperature. The salt of the triethylamine hydrochloride was filtered off, and the solvent was distilled at 100 °C under reduced pressure. The remaining brown crystalline mass was taken up in ethyl acetate, treated with activated charcoal, and dried with magnesium sulfate. The solution was filtered and evaporated to dryness. The foamy solid was then redissolved in dichloromethane (50 mL), and the solution saturated with *n*-hexane. Both solvents were evaporated slowly at low temperature. The last procedure was repeated, and the remaining yellowish, foamy solid was vacuum dried at 70 °C (4.27 g, 75.7%): FAB m/z = 983 (100%) M^+ – peak, m/z = 843 (17%), m/z = 799 (30%), m/z = 512 (14%); mp 100.7 °C; ^{1}H NMR (360 MHz, $CDCl_3$) δ = 4.40 (s, 2 H br, aliphatic protons), 4.68 (s, 2 H br, aliphatic protons), 6.97–7.33 (m, 7 H), 7.72 (dxd, 1 H), 7.86 (d, 1 H), 8.31 (t, 2 H br), 8.58 (s, 1 H), 8.75 (s, 1 H). Elemental Anal. found % (calcd for $C_{69}H_{67}N_9O_4$ included 1 mol of hexane and 1 mol of water): C, 76.5 (76.3); H, 5.9 (6.2); N, 11.9 (11.9).

The ligand **2** was prepared with the procedure shown in Scheme II. A mixture of 1,3,5-tris[4-((benzylamino)methyl)phenyl]benzene[21] (2.0 g, 3.0 mmol) and triethylamine (1.01 g, 10 mmol) in 10 mL of dimethylformamide was added to a stirred mixture of 2,2′-bipyridine-5-acid chloride (2.0 g, 10 mmol) in dimethylformamide (25 mL). Stirring was continued overnight, and after evaporation of the solvent the residue was dissolved in chloroform. The chloroform layer was concentrated in vacuo and chromatographed on alumina with chloroform to afford nearly pure **2**. For final purification the compound was recrystallized in an ethylacetate/cyclohexane mixture (1.9 g, 55%): FAB m/z = 1210.4 (MH^+, 100%; calc 1210.5), 1119.4 (MH^+ – benzyl, 2%), 1026.4 (M^+ – bpyCO, 29%); mp 123–127 °C; ^{1}H NMR (200 MHz $CDCl_3$) δ = 4.53 (6 H, Ar-CH_2), 4.82 (6 H, Ar-CH_2), 7.15–7.45 (m, 24 H, 21 Ar-H, 3 bpy-H), 7.68–7.76 (m, 6 H, Ar-H), 7.79–7.84 (m, 3 H, Ar-H), 7.82 (td, 3 bpy-H, ^3J = 7.8 Hz, ^4J = 1.8 Hz), 7.97 (dd, 3 bpy-H, ^3J = 8.2 Hz, ^4J = 2.2 Hz), 8.38 (dt, 3 bpy-C-H, ^3J = 7.8 Hz, ^4J = 1.0 Hz), 8.44 (dd, 3 bpy-H, ^3J = 8.2 Hz, ^4J = 0.7 Hz), 8.67 (ddd, 3 bpy-H, ^3J = 4.8 Hz, ^4J = 1.8 Hz, ^4J = 1.0 Hz), 8.86 (dd, 3 bpy-H, ^4J = 2.2 Hz, ^4J = 0.7 Hz); ^{13}C NMR (22.62 MHz, $CDCl_3$) δ = 47.42 (CH_2), 51.40 (CH_2), 120.70, 121.38 (CH), 124.23 (CH), 125.20 (CH), 127–129 (8 CH), 131.64 (C), 135.62 (CH), 136.46 (CH), 137.01 (CH), 140.57 (C), 141.90 (C), 147.18 (CH), 149.35 (CH), 155.20 (C), 157.21 (C), 169.90 (CO); IR 710 (m), 770 (s), 820 (w), 1005 (m), 1165 (m), 1260–1320 (m), 1435 (s), 1460 (s), 1600 (s), 1650 (vs), 2980–3020 (w).

The ligand **3** was prepared by the reaction sequence illustrated in Scheme III. The starting compound 4-acetyl-4′-methylbiphenyl has been prepared according to Byron et al.[22] The acid chloride of 2,2′-bipyridine used in the last step has been obtained according to Belser.[23] Elemental Anal. found % (calcd for $C_{99}H_{75}N_9O_3 \cdot 0.5CHCl_3$): 80.11 (79.76), 5.08 (5.08), 8.57 (8.41).

1,3,5-Tris[4-(4′-methylphenylyl)phenyl]benzene (**4**) was prepared as follows. A solution containing 8.00 g (0.038 mol) of **1** in 100 mL of chloroform and 5.24 g (0049 mol) trimethyl orthoformate was cooled to 0 °C and saturated with anhydrous hydrogen chloride for 2 h. The bubbling was continued for 4 h at ambient temperature. The dark solution was evaporated to dryness. The remaining solid was washed several times with cold ethanol and recrystallized from toluene, 3.00 g (41%) of **4**: mp 140–142 °C; ^{1}H NMR (200 MHz, $CDCl_3/TMS_{int}$) δ = 2.45 (s, 9 H, ar-CH_3), 7.31 (d, 6 H, Ar-H), 7.6 (d, 6 H, Ar-H), 7.81 (d, 6 H, Ar-H), 7.9 (s, 3 H, Ar-H); ^{13}C NMR (50.32 MHz, $CDCl_3/TMS_{int}$) δ = 137.29, 137.79, 139.78, 140.41, 142.04 (C), 124.96, 126.97, 127.75, 129.65 (CH), 21.22 (CH_3); $C_{45}H_{36}$ (576.8); FAB m/z 576 (100%) (M^+); 288 (24%) (M^{2+}); 91 (5%) ($C_7H_7^+$). Elemental Anal. found % (calcd for $C_{45}H_{36}$): 93.72 (93.71), 6.29 (6.29).

1,3,5-Tris[4-(4′-(bromomethyl)phenylyl)phenyl]benzene (**5**) was obtained as follows. **4** (2.00 g, 3.47 mmol) and 1.96 g (11 mmol) of *N*-bromosuccinimide, NBS, were dissolved in tetrachloromethane and

(17) Kröhnke, F.; Zecher, W. *Angew. Chem.* **1962**, *74*, 811. Kröhnke, F.; Gross, K. F. *Chem. Ber.* **1959**, *42*, 22.
(18) Kröhnke, F. *Angew. Chem.* **1963**, *74*, 181. Huang, T. L. J.; Brewer, D. G. *Can. J. Chem.* **1981**, *59*, 1689.
(19) Black, G.; Depp, E.; Corson, B. B. *J. Org. Chem.* **1949**, *14*, 14.
(20) Grammenudi, S.; Franken, M.; Vögtle, F.; Steckhan, E. *J. Inclusion Phenom.* **1987**, *5*, 695.
(21) Ebmeyer, F.; Vögtle, F. *Angew. Chem.* **1989**, *101*, 95. Sendhoff, N.; Kissener, W.; Vögtle, F.; Franken, S.; Puff, H. *Chem. Ber.* **1988**, *121*, 2179.
(22) Byron, D. J.; Gray, G. W.; Wilson, R. C. *J. Chem. Soc.* **1966**, 840.
(23) Belser, P., unpublished results. See also refs 17–19.

refluxed under irradiation. The solution was filtered hot and evaporated. The residue was dissolved in CH_2Cl_2 and washed with $NaHCO_3$ solution and water. The organic layer was dried over $MgSO_4$ and evaporated to dryness. For purification the remaining solid was recrystallized several times from toluene: 2.1 g (74%) of **5**, mp 134–136 °C; ^{1}H-NMR (200 MHz, $CDCl_3/TMS_{int}$) δ = 4.6 (s, 6 H, CH_2Br), 7.5 (d, 6 H, Ar-H), 7.65 (d, 6 H, Ar-H), 7.7 (d, 6 H, Ar-H), 7.8 (d, 6 H, Ar-H), 7.9 (s, 3 H, Ar-H); ^{13}C NMR (50.32 MHz, $CDCl_3/TMS_{int}$) δ = 137.06, 139.75, 140.29, 140.8, 141.96 (C), 125.12, 127.53, 127.65, 127.86, 129.7 (CH), 33.44 (CH_2Br); $C_{45}H_{33}Br_3$, (813.5); MS (EI, m/z), 814 (45%) (M^+); 82 (94%) (HBr^+). Elemental Anal. found % (calcd for $C_{45}H_{35}Br_3O$, included 1 mol water): 65.01 (65.00), 4.06 (4.24).

1,3,5-Tris{4-[4′-((*N*-benzylamino)methyl)phenylyl]phenyl}benzol (**6**) was obtained in the following way. A suspension of 1.50 g (1.84 mmol) of **5** and 5.50 g of sodium carbonate in 60 mL of benzylamine was stirred for 36 h. The suspension was filtered, and the filtrate was evaporated. The residue was treated with 20 mL of 6 N hydrochloric acid, heated under reflux for 30 min, and filtered. The remaining solid was poured into diluted sodium hydroxide solution. The mixture was extracted with CH_2Cl_2, and the organic fractions were separated, washed with water, and dried over $MgSO_4$. The solvent was removed, and the residue was separated by silica gel column chromatography (eluent: toluene/methanol 10:1) 0.45 g (27%) of **6**, mp 166–168 °C; ^{1}H-NMR (200 MHz, $CDCl_3/TMS_{int}$) δ = 3.87 (s, 6 H, NCH_2), 3.87 (s, 6 H, NCH_2), 7.45 (d, 6 H, Ar-H), 7.64 (d, 6 H, Ar-H), 7.72 (d, 6 H, Ar-H), 7.8 (d, 6 H, Ar-H), 7.88 (s, 3 H, Ar-H), 7.27–7.4 (m, 15 H, Ar-H); ^{13}C NMR (50.32 MHz, $CDCl_3/TMS_{int}$) δ = 130.43, 139.35, 139.66, 139.96, 140.29, 142.03 (C), 125.04, 127.07, 127.14, 127.57, 127.79, 128.25, 128.5, 128.76 (C), 52.86, 53.24 (CH_2), $C_{66}H_{57}N_3$ (892.2); MS (EI, m/z) 891, (18%) (M^+); 786, (51%) ($M^+ - C_7H_7N$); 681, (40%) ($M^+ - 2C_7H_7N$).

1,3,5-Tris[4-((((2,2′-bipyridyl-5-ylcarbonyl)benzylamino)methyl)-phenylyl)phenyl]benzene **3** was prepared (Scheme III) as follows. A mixture of 0.40 g (0.448 mmol) of amine **6** and 2 mL of triethylamine in 20 mL of dimethylformamide was added to a stirred mixture of 2,2′-bipyridine–5-acid chloride (0.50 g, 2.29 mmol) in dimethylformamide. The mixture was heated for 10 min to 80 °C. Stirring was continued overnight, and after evaporation of the solvent the residue was dissolved in chloroform. The organic layer was concentrated in vacuo and chromatographed on silica gel (eluent, chloroform–methanol–aqueous ammonia 300:10:1) to afford **3**. For final purification the compound was recrystallized in a toluene/ethanol mixture: 250 mg (39%) of **3**, mp 144 °C; ^{1}H-NMR (200 MHz, CD_2Cl_2/TMS_{int}) δ = 4.55 (s, 6 H, N-CH_2), 4.79 (s, 6 H, N-CH_2), 7.2–7.48 (m, 15 H, Ar-H), 7.31 (ddd, 3 H, bpy-H), 7.37 (d, 6 H, Ar-H), 7.72 (d, 6 H, Ar-H), 7.78 (d, 6 H, Ar-H), 7.79 (ddd, 3 H, bpy-H), 7.88 (d, 6 H, Ar-H), 7.95 (s, 3 H, Ar-H), 7.97 (dd, 3 H, bpy-H), 8.42 (ddd, 3 H, bpy-H), 8.48 (dd, 3 H, bpy-H), 8.65 (ddd, 3 H, bpy-H), 8.83 (dd, 3 H, bpy-H); ^{13}C NMR (50.32 MHz, CD_2Cl_2/TMS_{int}) δ = 127.130 (2C), 132.2, 136.5, 140.2, 140.3, 142.2, 155.5, 157.3, 170.0 (C), 120.8, 121.4, 124.5, 125.2 (CH), 127–129 (7 CH), 135.8, 137.3, 147.5, 149.6 (CH), 47.9, 51.8 (CH_2), $C_{99}H_{75}N_9O_3$ (1437.6); MS (FAB, m/z), 1439.4 (MH^+).

Preparation of the Metal Complexes. The metal complexes of the ligands **1** and **2** were prepared according to the general reaction

$$x[M(bpy)_2Cl_2] + \mathbf{1, 2, or 3} \xrightarrow[\text{excess } NH_4PF_6]{\uparrow\downarrow\text{ethylene glycol}} \mathbf{(1, 2, or 3)}[M(bpy)_2]_x(PF_6)_{2x} \quad (1)$$

$$x = 1, 2, 3;\ M = Ru, Os$$

With ligand **3**, the only complex synthesized was **3**·$\mathbf{Ru_3}$ because the insolubility of the ligand and its complexes precluded the chromatographic purification. Reaction 1 was carried out in ethylene glycol/diluted hydrochloric acid at 120 °C (140 °C for the osmium complexes) for several hours. The solvent was then evaporated, and the complexes dissolved in water and precipitated as PF_6^- salts by addition of ammonium hexafluorophosphate (for details, see later). The compounds were purified according to the following methods: (a) chromatography on partially deactivated aluminium oxide (this method was only applicable to mononuclear complexes); (b) chromatography on silica gel; (c) preparative thin-layer plates (PTLC) (silica gel); (d) recrystallization from an acetonitrile/diethyl ether mixture (vapor diffusion method).

The mixed-metal (Ru–Os) complexes were prepared in a stepwise manner as shown in Scheme IV. The preparation of **1**·$\mathbf{Ru_2Os}$ and **2**·$\mathbf{Ru_2Os}$, was performed starting from the corresponding mononuclear Os compound. It should be noticed that in the last step of the reaction all possible trinuclear complexes (Ru,Ru,Ru; Ru,Ru,Os; Ru,Os,Os; Os,Os,Os) might be produced, in principle, due to the exchange of the $M(bpy)_2$ units (M = Ru, Os). In order to investigate this possibility, the stability of the trinuclear metal complexes was tested under the reaction condition. An equimolar amount of **1**·$\mathbf{Ru_3}$ and **1**·$\mathbf{Os_3}$ was mixed and heated up for 20 h at 120 °C in ethylene glycol. The emission spectra recorded before and after the treatment were identical, suggesting that the exchange of the $M(bpy)_2$ units can be ruled out.

Scheme IV

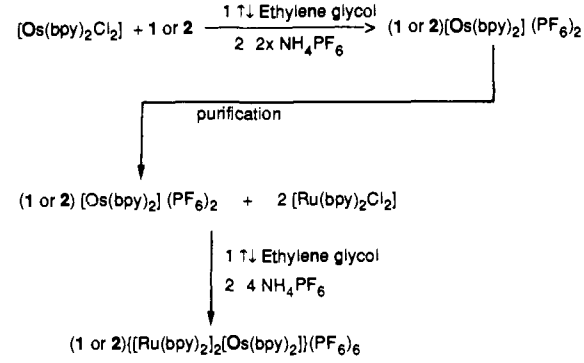

All the metal complexes were characterized by ^{1}H NMR spectra, fast atomic bombardment mass spectra (FAB), electrospray ionization spectra, IR, cyclic voltammetry, (CV), and elemental analysis (only for the complexes of **1**; the other complexes are too big to give meaningful results). The use of electrospray in the place of FAB for some compounds was dictated by practical reasons related to working conditions of the external laboratory where such measurements were performed.

1$[Ru(bpy)_2](PF_6)_2 \equiv$ **1**·**Ru**. $Ru(bpy)_2Cl_2 \cdot 2H_2O$ (0.052 g, 0.1 mmol) dissolved in 10 mL of ethanol was added during a 1-h period to a solution of **1**, 0.1 g (0.1 mmol) in 10 mL of ethylene glycol/1 mL of 0.2 molar hydrochloric acid at 100 °C under reflux. The ethanol was then evaporated, and the temperature rose to 120 °C. The reaction mixture was held at this temperature for 3 h. The course of the reaction was followed by TLC. The solvents were evaporated under reduced pressure, and the remaining metal complex was taken up in hot water, filtered, and precipitated at 25 °C with an excess of a solution containing ammonium hexafluorophosphate. The orange solid was collected, washed with cold water at 0 °C, and dried at 100 °C under reduced pressure. The complex was purified on a aluminium oxide column. The used aluminium oxide was first deactivated with 2.5% of water. The complex was eluted with acetone/water (49:1). The solution containing the metal complex was then evaporated to dryness, and the solid was dissolved again in the minimum amount of acetonitrile. By means of a slow vapor diffusion of diethyl ether (in a closed system) into the acetonitrile solution, the compound crystallized out in a pure form: orange, microcrystalline solid (0.093 g, yields 53.3%); FAB m/z = 1541 (82%) $M^+ - PF_6^-$; m/z = 1395 (100) $M^+ - 2PF_6^-$; CV $E_{1/2}$ ($E_a - E_p$) [mV] +1300 (70), −1210 (70), −1515 (70), −1735 (70); ^{1}H NMR (360 MHz, acetonitrile-*d*): For this as well as for the other compounds, the spectra were recorded at 72 °C in order to have a better resolution. The aromatic region was too complicated to be assigned. In each case, correlation between aliphatic (two different $-CH_2-$ groups) and aromatic protons was performed. For this complex the ratio of the aliphatic protons to the aromatic protons is 12:55 (calc 12:55). Elemental Anal. found % (calcd for $C_{83}H_{77}F_{12}N_{13}O_8P_2Ru$ included 5 mol water): C, 56.1 (56.0); H, 4.3 (4.3); N, 10.2 (10.1).

1$\{[Ru(bpy)_2]_2\}(PF_6)_4 \equiv$ **1**·$\mathbf{Ru_2}$. The procedure for the preparation of the compound was the same as described above with the exception that the hydrochloric acid was 0.1 molar. The complex was purified on a silica gel 60 column (diameter 7 cm, length 20 cm) *N*,*N*-dimethylformamide/water/ammonium chloride (1:1:0.04) as eluting solvent. The main orange band containing the dinuclear metal complex was collected and the solution evaporated to dryness. The remaining solid was dissolved in a small amount of water, and the complex was precipitated with ammonium hexafluorophosphate. The solid was then dried and recrystallized with acetonitrile/diethyl ether: orange solid (0.067 g, 28%); FAB m/z = 2244 (40%) $M^+ - PF_6^-$; m/z = 2098 (100%) $M^+ - 2PF_6^-$; CV $E_{1/2}$($E_a - E_p$) [mV] +1300 (80), −1190 (80); ^{1}H NMR (360 MHz, acetonitrile-*d*) the ratio of the aliphatic protons to the aromatic protons of the complex is 12:70 (calc 12:71). Elemental Anal. found % (calcd

for $C_{105}H_{96}F_{24}N_{18}O_8P_4Ru_2$ included 5 mol water and 1 mol acetonitrile): C, 50.1 (50.1); H, 3.9 (3.8); N, 9.8 (10.0).

1{[Ru(bpy)$_2$]$_3$}(PF$_6$)$_6$ ≡ **1·Ru$_3$**. The route of preparation and purification was the same as described for the complex **1**{[Ru(bpy)$_2$]$_2$}(PF$_6$)$_4$, but no hydrochloric acid was added. The following additional purification procedure yielded an analytically pure sample: portions (0.015 g) of the complex were put on a preparative thin-layer plate (20 × 20 cm, 2 mm silica gel 60) and then developed with the solvent system of *N*,*N*-dimethylformamide/water/ammonium hexafluorophosphate (1:1:0.04). The plate was then dried in a furnace at 60 °C. The well separated band containing the complex was scratched from the plate, dispersed in acetone, and poured into a column. The complex was then washed out with a solution of 4% ammonium hexafluorophosphate dissolved in acetone/water (1:0.01). Water was added to the solution, and the acetone was distilled off. The precipitated metal complex was collected and vacuum dried at 100 °C: orange-brown solid (0.21 g, 68%); FAB m/z = 2947 (34%) $M^+ + PF_6^-$; m/z = 2802 (38%) $M^+ - 2PF_6^-$; m/z = 2656 (18%) $M^+ - 3PF_6^-$; CV $E_{1/2}(E_a - E_p)$ [mV] +1310 (80), −1180 (80); ^{1}H NMR (360 MHz, acetonitrile-*d*) the ratio of the aliphatic protons of the aromatic protons of the complex is 12:87 (calcd 12:87). Elemental Anal. found % (calcd for $C_{127}H_{117}F_{36}N_{21}O_8P_6Ru_3$ included four water and one mol diethyl ether) C, 47.0 (47.1); H, 3.6 (3.6); N, 9.2 (9.1).

1{[Ru(bpy)$_2$]$_2$[Os(bpy)$_2$]}(PF$_6$)$_6$ ≡ **1·Ru$_2$Os**. **1·Os** (0.05 g, 2.82 × 10^{-5} mol) and 0.031 g (6.0 × 10^{-5} mol) of [Ru(bpy)$_2$Cl$_2$]·2H$_2$O were dissolved in a mixture of 5 mL of ethylene glycol and 0.5 mL of water and heated up to 140 °C for 3 h. The solvents were evaporated, and the olive-brown solid was taken up with 10 mL of water, filtered, and subsequently precipitated with an excess of ammonium hexafluorophosphate. The compound was then dried under reduced pressure at 100 °C. The purification was done in the same manner described for the other complexes: yields 0.026 g (29.0%); FAB m/z = 3036 (75%) $M^+ - PF_6^-$; m/z = 2891 (54%) $M^+ - 2PF_6^-$; m/z = 2745 (18%) $M^+ - 3PF_6^-$; CV $E_{1/2}(E_a - E_p)$ [mV] +1300 (90) 2Ru, +865 (75) 1Os, −1160 (110); ^{1}H NMR (360 MHz, acetonitrile-*d*) the ratio of the aliphatic protons to the aromatic protons of the complex is 12:86 (calcd 12:87).

1{[Os(bpy)$_2$]$_3$}(PF$_6$)$_6$ = **1·Os$_3$**. The preparation of this compound was carried out as described for **1**{[Ru(bpy)$_2$]$_3$}(PF$_6$)$_6$. The heating period (140 °C) was prolongated to 12 h: yields 0.027 g (28%); CV $E_{1/2}(E_a - E_p)$ [mV] +870 (90), −1140 (80); ^{1}H NMR (300 MHz, acetonitrile-*d*) the ratio of the aliphatic protons to the aromatic protons of the complex is 12:90 (calcd 12:87).

The preparations of the metal complexes with the ligand **2** were performed with the same procedure described above for the compounds with the ligand **1**.

2{[Ru(bpy)$_2$]$_3$}(PF$_6$)$_6$ ≡ **2·Ru$_3$**. A preparation of a 7.53 × 10^{-5} molar scale on **2** has given 0.03 g (25%) of the orange complex. Electrospray m/z = 408.4 (100%) M − 6PF$_6^-$/6; m/z = 519.1 (61%) M − 5PF$_6^-$/5; m/z = 685.2 (29%) M − 4PF$_6^-$/4; m/z = 961.9 (23%) M − 3PF$_6^-$/3; CV $E_{1/2}(E_a - E_p)$ [mV] +1310 (95), −1165 (70); ^{1}H NMR (360 MHz, acetonitrile-*d*) the ratio of the aliphatic protons to the aromatic protons of the complex is 12:99 (calcd 12:99).

2[Os(bpy)$_2$](PF$_6$)$_2$ ≡ **2·Os** (Precursor of **2·Ru$_2$Os**). A preparation in a 2.0 × 10^{-5} molar scale on **2** has given 0.014 g of an olive solid (35%); FAB m/z = 1857 (90%) $M^+ - PF_6^-$; m/z = 1714 (98%) $M^+ - 2PF_6^-$; CV $E_{1/2}(E_a - E_p)$ [mV] +880 (60), −1135 (70); ^{1}H NMR (360 MHz, acetonitrile-*d*) the ratio of the aliphatic protons to the aromatic protons of the complex is 12:67 (calcd 12:67).

2{[Os(bpy)$_2$]$_3$}(PF$_6$)$_6$ ≡ **2·Os$_3$**. A preparation in a 2.0 × 10^{-5} molar scale has given 0.017 g (24%) of a dark olive solid. Electrospray m/z = 453.3 (100%) M − 6PF$_6^-$/6; m/z = 572.7 (34%) M − 5PF$_6^-$/5; m/z = 751.7 (7%) M − 4PF$_6^-$/4; m/z = 1050.6 (6%) M − 3PF$_6^-$/3; CV $E_{1/2}(E_a - E_p)$ [mV] +865 (70), −1150 (70); ^{1}H NMR (360 MHz, acetonitrile-*d*) the ratio of the aliphatic protons to the aromatic protons of the complex is 12:101 (calcd 12:99).

2{[Ru(bpy)$_2$]$_2$[Os(bpy)$_2$]}(PF$_6$)$_6$ ≡ **2·Ru$_2$Os**. A preparation in a 1 × 10^{-5} molar scale on [Os(bpy)$_2$(L$_2$)](PF$_6$)$_2$ has given 0.018 g (52.8%) of an olive green solid. Electrospray m/z = 423.2 (100%) M − 6PF$_6^-$/6; m/z = 537.0 (58%) M − 5PF$_6^-$/5; m/z = 707.1 (28%) M − 4PF$_6^-$/4; m/z = 991.6 (22%) M − 3PF$_6^-$/3; CV $E_{1/2}(E_a - E_p)$ [mV] +1310 (75) 2Ru, +880 (75) 1Os, −1140 (75); ^{1}H NMR (360 MHz, acetonitrile-*d*) the ratio of the aliphatic protons to the aromatic protons of the complex is 12:100 (calcd 12:99).

Oxidation with Ce(IV). A 0.049 N standard solution of ammonium cerium(IV) nitrate in HNO_3 (6%) was obtained from Aldrich. For the oxidation of the Os(II) complexes, the Ce(IV) solution was diluted 10 times with 2 M H_2SO_4. Three milliliters of 1.0 × 10^{-4} N solution in acetonitrile/H_2O (5:1 v/v) of the Os(II) complexes was titrated by adding μL aliquots of the Ce(IV) solution. For the oxidation of the Ru(II) complexes different conditions had to be used because the Ru(III) species are stable only in very acid solutions. The Ce(IV) standard solution was diluted 1:20 with 6% HNO_3, and the Ru(II) complexes were dissolved in 40:60 acetonitrile/nitric acid (6%) to obtain a 0.33 × 10^{-4} N solution. The titration was performed monitoring the change in absorbance in the visible region where the Ru(II) and Os(II) species exhibit an intense absorption band (Figure 3), whereas the absorbance of the Ru(III) and Os(III) species is very small.[24]

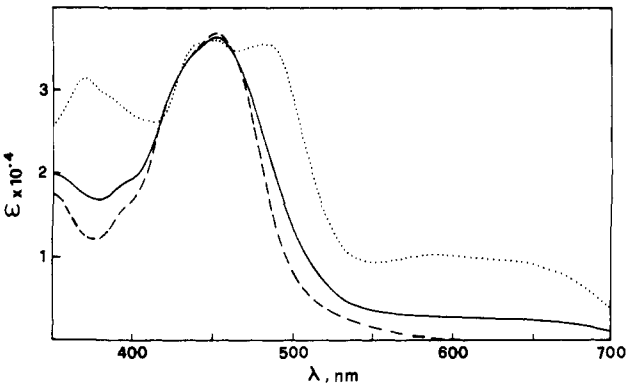

Figure 3. Room temperature absorption spectra of **1·Ru$_3$** (- -), **1·Os$_3$** (···), and **1·Ru$_2$Os** (—) in acetonitrile solution.

Results

All the compounds examined were stable in the solvents used both in the dark and under laboratory light. In order to check the stability of the complexes toward metal exchange under the preparative conditions, equimolar amounts (5 × 10^{-4} M) of **1·Ru$_3$** and **1·Os$_3$** were heated at 120 °C in ethylene glycol for 20 h. Formation of mixed-metal species would have caused a decrease in the luminescence intensity at 640 nm (vide infra). No change, however, was detected.

Absorption Spectra. The ligands **1**, **2**, and **3** are very soluble in CH_2Cl_2, but insoluble in net CH_3CN. In a 1:10 v/v CH_2Cl_2/CH_3CN mixture, these ligands exhibit strong absorption bands in the near UV region. The absorption spectrum of **1** shows the characteristic bands of the bpy units with maxima at 240 and 288 nm. In **2**, the bpy bands merge with the intense band of 1,3,5-triphenylbenzene (λ_{max} = 251 nm, ϵ = 61 000 M^{-1} cm^{-1})[24] yielding a broad band with maximum at 267 nm (ϵ = 107 000 M^{-1} cm^{-1}). In **3**, the bpy band at 288 nm is completely hidden by the very intense band of the spacer.[24] Its spectrum shows only a maximum at 292 nm (ϵ = 176 500 M^{-1} cm^{-1}). In all the complexes studied the ligand centered (LC) bands in the UV region are accompanied by the characteristic[2] metal-to-ligand charge-transfer (MLCT) bands in the visible (Table II). For illustration purposes, the visible spectra of **1·Ru$_3$**, **1·Os$_3$**, and **1·Ru$_2$Os** are displayed in Figure 3.

Luminescence. The ligands **1**, **2**, and **3** exhibit fluorescence bands (390, 368, 376 nm, respectively) in fluid solution at room temperature and both fluorescence and phosphorescence (for the latter, λ_{max} = 480, 480, and 495 nm, respectively) in rigid matrix at 77 K. These luminescence bands can no longer be observed in the metal complexes, including the monometallic and bimetallic species **1·Ru** and **1·Ru$_2$**. All the complexes examined are luminescent both in rigid matrix at 77 K and in fluid solution at room temperature. Some luminescence spectra are displayed in Figures 4 and 5. The luminescence properties of **1·Ru$_3$**, **1·Os$_3$**, **1·Ru$_2$Os**, **2·Ru$_3$**, **2·Os$_3$**, and **2·Ru$_2$Os** in aerated acetonitrile solution at room temperature are shown in Table III where the luminescence properties of the 2:1 stoichiometric mixtures of **1·Ru$_3$** and **1·Os$_3$**, and **2·Ru$_3$** and **2·Os$_3$** are also shown for comparison purposes (vide infra). The luminescent properties of **1·Ru**, **1·Ru$_2$**, and **3·Ru$_3$** are identical to those of **1·Ru$_3$** and therefore are not

Table II. Absorption Spectra[a]

	λ, nm (ε, M^{-1} cm^{-1})					
1·Ru				450(12400)		290 (94000)
1·Ru_2				451(24700)		290(149100)
1·Ru_3				450(38100)		290(208900)
1·Os_3	642 (9500)	588(9700)	478(33900)	450(34700)	370(30000)	290(247700)
1·Ru_2Os				450(36300)		289(218900)
2·Ru_3				450(37300)		287(230800)
2·Os_3	642(8800)	589(9700)	478(33500)	449(34100)	370(29600)	290(273300)
2·Ru_2Os				450(35330)		288(232900)
$Ru(bpy)_3^{2+}$ [b]				452(14600)		288(76600)
$Os(bpy)_3^{2+}$ [b]		579(3270)	478(11100)	436(10700)		290(78000)

[a] Room temperature, acetonitrile solution. [b] Reference 2.

Table III. Luminescence Properties

	298 K[a]						77 K[b]			
	Ru			Os			Ru		Os	
	λ_{max}, nm	τ, ns	I_{rel}	λ_{max}, nm	τ, ns	I_{rel}	λ_{max}, nm	τ, μs	λ_{max}, nm	τ, μs
1·Ru_3	640	200	100				595	4.2		
1·Os_3				780	25	100			720	0.68
$^2/_3$(**1·Ru_3**) + $^1/_3$(**1·Os_3**)	640	190	64	*c*	*c*	*c*	595	3.5	720	
1·Ru_2Os	642	185	2.5	780	24	98	595	*d*	720	0.70
2·Ru_3	640	210	100				595	4.4		
2·Os_3				780	25	100			720	0.67
$^2/_3$(**2·Ru_3**) + $^1/_3$(**2·Os_3**)	640	200	63	*c*	*c*	*c*	595	4.0	720	
2·Ru_2Os	640	200	31	*c*	*c*	80	595	4.0	720	0.60
$Ru(bpy)_3^{2+}$	615	170					582	4.8		
$Os(bpy)_3^{2+}$				743[e]	60[e]				710	0.83

[a] Aerated acetonitrile solution. [b] Propionitrile–butyronitrile solution. [c] Not measurable because it is covered by the much more intense Ru-based emission. [d] Not measurable because of strong overlap with the more intense Os-based emission. [e] From: Kober, E. K.; Caspar, J. V.; Lumpkin, R. S.; Meyer, T. J. *J. Phys. Chem.* **1986**, *90*, 3722.

reported in Table III. At 77 K the homonuclear Ru and Os complexes show emission maxima at 595 nm (4.2 μs) and 720 nm (0.68 μs), respectively.

The procedure used to obtain values for the quenching of the luminescence of the Ru-based components and the sensitization of the luminescence of the Os-based component in the mixed-metal compounds was as follows (for the sake of simplicity, we will only describe the case of **1·Ru_2Os**; the same procedure was used for **2·Ru_2Os**). First, we have recorded the absorption spectra of equimolar (1.0×10^{-5} M) solutions of **1·Ru_2Os** and of the **1·Ru_3** and **1·Os_3** "parent" compounds, and we have found that they exhibit an isosbestic point at 461 nm (Figure 3). Then, solutions of **1·Ru_2Os** and of a 2:1 mixture of **1·Ru_3** and **1·Os_3** having the same concentrations were prepared and were found to exhibit identical absorption spectra. The luminescence spectra of such solutions were recorded with excitation in the isosbestic point at 461 nm under identical instrumental conditions. The quenching of the Ru-based luminescence was obtained by comparing the heights of the emission bands at 640 nm where the luminescence of the Os-based unit is negligible (Figure 4).

In order to measure the sensitization of the luminescence of the Os-based unit, a more complex procedure had to be adopted because the tail of the (residual) luminescence of the Ru-based units strongly interferes with the measurement of the luminescence intensity of the Os-based units even at their emission maximum (Figure 4). The luminescence spectra of the **1·Ru_2Os** and **1·Os_3** compounds were recorded with excitation in their isosbestic point at 461 nm. From the luminescence band of **1·Ru_2Os**, the contribution coming from the (unquenched) luminescence of the Ru-based units was substracted by using a normalized (at 640 nm) spectrum of **1·Ru_3** (Figure 4). The difference in the heights of the **1·Ru_2Os** and **1·Ru_3** bands at 780 nm measures the contribution of the Os-based unit to the **1·Ru_2Os** luminescence at that wavelength and can be directly compared with the height of the **1·Os_3** band.

The luminescence decay was always monoexponential under the experimental conditions used.

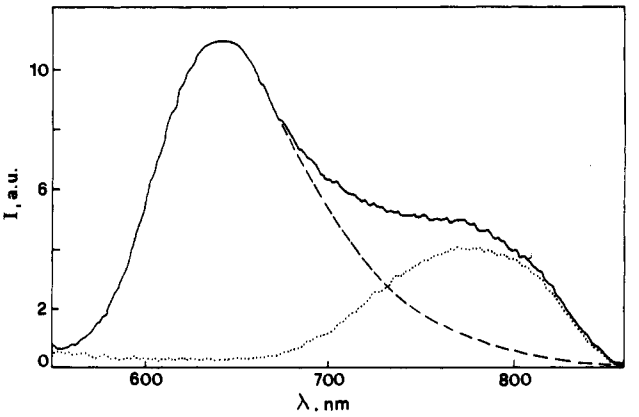

Figure 4. Room temperature luminescence spectra of isoabsorptive (λ_{exc} = 461 nm) acetonitrile solutions of **1·Ru_2Os** (—), **1·Os_3** (···), and **1·Ru_3** (- -). The last spectrum has been normalized to the maximum of the **1·Ru_2Os** spectrum.

Electrochemical Properties. The electrochemical redox potentials of the investigated complexes are collected in Table IV.

Generation of Mixed-Valence Compounds. Addition of the standardized Ce(IV) solution to 10^{-4} N solutions of $Ru(bpy)_3^{2+}$, **1·Ru_3**, and **2·Ru_3** (see Experimental Section) caused strong spectral changes in the absorption spectra, as expected for the oxidation of Ru(II) and Os(II) bipyridine-type complexes.[25] The absorbance at 450 nm (MLCT band of the Ru(II) complexes) decreased linearly with increasing number of added oxidation equivalents (Figure 6). A parallel decrease of the luminescence intensity was observed for the $Ru(bpy)_3^{2+}$ solution, whereas the decrease of the luminescence intensity was not linear for **1·Ru_3** and **2·Ru_3**

(24) Berlman, I. B. *Handbook of Fluorescence Spectra of Aromatic Molecules*; Academic Press: New York, 1971.

(25) $Ru(bpy)_3^{3+}$ and $Os(bpy)_3^{3+}$ show the lowest energy (doublet → doublet) absorption band at 676 and 563 nm, respectively, with small molar absorption coefficients (409 and 585 M^{-1} cm^{-1}, respectively). See: Bryant, G. M.; Fergusson, J. E. *Austr. J. Chem.* **1971**, *24*, 275.

Table IV. Electrochemical Data[a]

	redox potential, V (relative current intensity)		
	oxidation		
	Ru	Os	reduction
1.Ru	+1.30(1)		-1.21
1.Ru$_2$	+1.30(2)		-1.19
1.Ru$_3$	+1.31(3)		-1.18
1.Os$_3$		+0.870(3)	-1.14
1.Ru$_2$Os	+1.30(2)	+0.865(1)	-1.16
2.Ru$_3$	+1.31(3)		-1.17
2.Os$_3$		+0.865(3)	-1.15
2.Ru$_2$Os	+1.31(2)	+0.880(1)	-1.14
Ru(bpy)$_3^{2+}$ [b]	+1.26		-1.35
Os(bpy)$_3^{2+}$ [b]	+0.83		-1.28

[a] Room temperature acetonitrile solution; potential values vs SCE; the second and third reduction processes are irreversible except for **1.Ru**. [b] Reference 2.

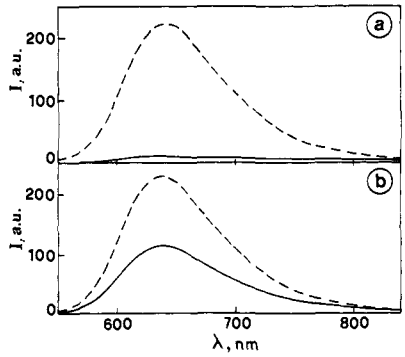

Figure 5. Room temperature luminescence spectra of isoabsorptive (λ_{exc} = 461 nm) acetonitrile solutions of (a) **1·Ru$_2$Os** (—) and a 2:1 mixture of **1·Ru$_3$** and **1·Os$_3$** (- -) and (b) **2·Ru$_2$Os** (– –) and a 2:1 mixture of **2·Ru$_3$** and **2·Os$_3$** (- -).

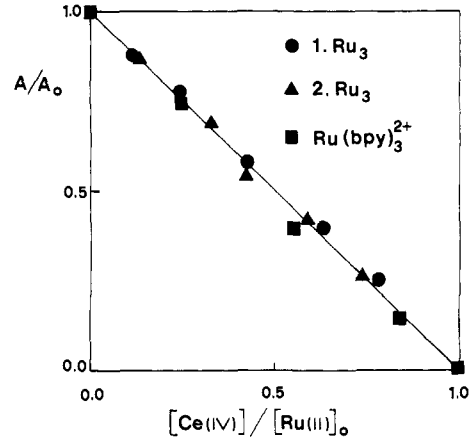

Figure 6. Changes in absorbance (λ = 450 nm) for a 1.0 × 10^{-4} M solution of Ru(bpy)$_3^{2+}$ and 0.33 × 10^{-4} M solutions of **1·Ru$_3$** and **2·Ru$_3$** upon addition of Ce(IV).

(Figure 7). The oxidized solutions were stable for limited time periods and recovered the original absorption and luminescence spectrum in a few hours. In the case of **3·Ru$_3$**, the oxidized solutions were unstable even for very short time periods, so that no reliable results could be obtained.

For Os(bpy)$_3^{2+}$, **1·Os$_3$**, and **2·Os$_3$** oxidation caused again a linear decrease in absorbance with increasing number of added oxidation equivalents. The changes in the luminescence intensity upon oxidation for the three compounds are shown in Figure 8. Absorption measurements in the near-infrared spectral region on a 3.3 × 10^{-4} M solution of **1·Os$_3$** containing 1.6 × 10^{-4} N Ce(IV) showed that no absorption band with $\epsilon > 50$ M^{-1} cm^{-1} was present in the range 800–1400 nm. The same result was

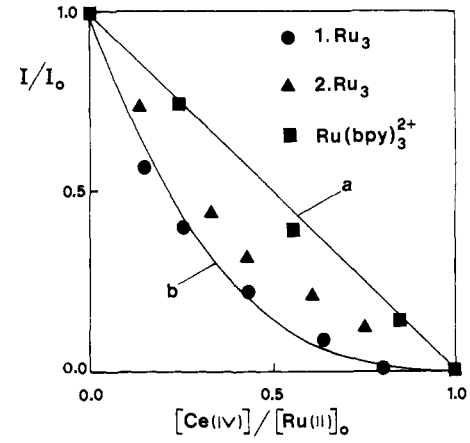

Figure 7. Changes in the luminescence intensity (λ = 640 nm) for a 1.0 × 10^{-4} M solution of Ru(bpy)$_3^{2+}$ and 0.33 × 10^{-4} M solutions of **1·Ru$_3$** and **2·Ru$_3$** upon addition of Ce(IV). For more details see text.

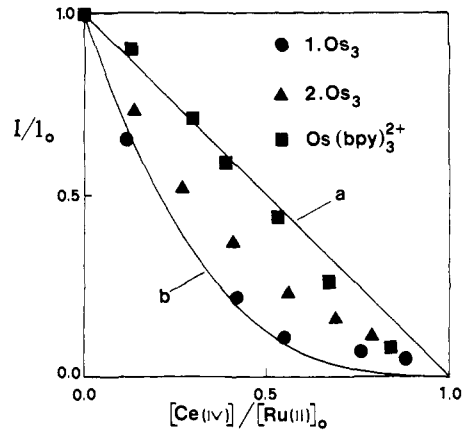

Figure 8. Changes in the luminescence intensity (λ = 780 nm) for a 3.0 × 10^{-4} M solution of Os(bpy)$_3^{2+}$ and 1.0 × 10^{-4} M solutions of **1·Os$_3$** and **2·Os$_3$** upon addition of Ce(IV). For more details see text.

recently obtained for similar mixed-valence systems studied by Haasnoot et al.[7g]

Discussion

Intercomponent Interactions. Extensive investigations on mono- and oligonuclear Ru(II) and Os(II) complexes[2,5,6] have shown that (i) oxidation is metal centered; (ii) Os(II) is easier to oxidize than Ru(II); (iii) reduction is ligand centered; (iv) the absorption bands in the visible region are due to spin-allowed metal-to-ligand charge-transfer (MLCT) transitions and related spin-forbidden bands for Os(II) complexes; and (v) luminescence takes place from the lowest energy excited state which is a formally triplet MLCT level. In oligonuclear complexes electronic interaction between the various components may range from very strong (with profound changes of the various properties on passing from mononuclear to oligonuclear species) to very weak (with almost equal properties for separated and bridged units).

An important thing to notice is that the first oxidation potential, the first reduction potential, the absorption maxima, and all the luminescence properties are identical (within the experimental errors) for **1·Ru**, **1·Ru$_2$**, and **1·Ru$_3$**. This suggests little or no electronic interaction between the identical metal-containing components that are present in **1·Ru$_2$** and **1·Ru$_3$**. Further confirmations of a very weak (if any) interaction come from (a) the identical absorption, luminescence, and redox properties exhibited by **1·Ru$_3$**, **2·Ru$_3$** and **3·Ru$_3$** and, respectively, by **1·Os$_3$** and **2·Os$_3$**; (b) the identical first oxidation and first reduction potentials of **1·Os$_3$**, **1·Ru$_2$Os**, **2·Os$_3$**, and **2·Ru$_2$Os**; and (c) the identical absorption spectrum exhibited by the mixed-metal

1·Ru$_2$Os and **2·Ru$_2$Os** complexes and by the 2:1 mixtures of their heterometallic "parent" trinuclear complexes. We can thus draw a general conclusion: the interaction of a $M(bpy)_2L^{2+}$ component (where L is the bpy-type coordinating site of the tripod ligands **1**, **2**, and **3**) with any other component which is present in the dinuclear and trinuclear supramolecular species is, at most, weak. The absence of intense ($\epsilon > 50$ M^{-1} cm^{-1}) intervalence bands in the mixed-valence **1·Os$_3$** compound confirms the lack of strong intercomponent interaction. It should be recalled, however, that even an interaction of a few cm^{-1} (which would of course be unnoticed in electrochemical experiments and intervalence-transfer absorption spectra) is sufficient to cause fast intercomponent energy and electron transfer.[5]

Properties of the Components. Each metal-containing component (Figure 2) can be viewed as a mixed-ligand complex since the coordination sites of the tripod ligands have properties slightly different from those of bpy because of the presence of an electron withdrawing amido group. This is the reason why the properties of $Ru(bpy)_2L^{2+}$ and $Os(bpy)_2L^{2+}$ are not identical to those of $Ru(bpy)_3^{2+}$ and $Os(bpy)_3^{2+}$, respectively. These differences consist of (a) a less negative first reduction potential, since the coordination sites of **1** or **2** are slightly easier to reduce than bpy; (b) a higher oxidation potential, since the metal ion in $M(bpy)_2L^{2+}$ is slightly more positive than in $M(bpy)_3^{2+}$ owing to the presence of the electron withdrawing substituent in L; (c) some slight differences in the shape of the absorption bands in the visible, caused by the presence of two MLCT transitions in the $M(bpy)_2L^{2+}$ components (M → L at lower energy, and M → bpy at higher energy); (d) a slight red shift of the luminescence in going from $M(bpy)_3^{2+}$ to $M(bpy)_2L^{2+}$, since in the latter species the lowest MLCT level involves the tripod ligand; (e) a slightly shorter lifetime at 77 K, because of the smaller energy gap between ground state and luminescent level; (f) a slightly longer lifetime in fluid solution at room temperature in the case of the Ru compounds, because of the slightly higher energy gap between luminescent level and the upper lying, short-lived triplet ligand field level; and (g) a greater sensitivity to the environment as shown by the red shift of the luminescence band with increasing solvent polarity. For **1·Ru$_3$**, λ_{max} is 636, 640, and 651 nm in dichloromethane (dielectric constant = 8.9), acetonitrile (37.4), and methylformamide (182.4), respectively.

Energy Transfer in 1·Ru$_2$Os and 2·Ru$_2$Os. As one can see from Figure 5, in acetonitrile solution the luminescence intensity of the Ru-based components in **1·Ru$_2$Os** and **2·Ru$_2$Os** is quenched to 4% and 50%, respectively (compare the I_{rel} value of the two compounds with those of the corresponding 2:1 mixture of the parent trinuclear homometallic species, Table III). In polypyridine complexes, Os(II) is easier to oxidize than Ru(II) (Table IV). Therefore, for complexes of the same ligands the MLCT levels lie at higher energy in the Ru(II) than in the Os(II) complexes. For our compounds, the excited-state energy of the Ru-based components is 2.08 eV and that of the Os-based components is 1.72 eV.[26] Therefore, the free energy change (neglecting entropy changes) for energy transfer from an excited Ru-based component to a ground-state Os-based component is approximately −0.36 eV. This thermodynamically favored process could account for the observed quenching.

In principle, fast excited state quenching can also occur by electron transfer.[2a] From the excited-state energy of the Ru-based components (2.08 eV) and the redox potentials shown in Table IV, it can be estimated that the reductive quenching process of the excited Ru-based component by the ground-state Os-based component is nearly isoergonic, and the oxidative quenching process is strongly endoergonic. Therefore, it seems unlikely that quenching by electron transfer, which implies a noticeable reorganizational energy in polar solvents, can be fast enough in our systems to compete with quenching by energy transfer.

Following the procedure described above, which are based on a comparison of the (corrected) luminescence intensities at 780 nm of **1·Ru$_2$Os** and **2·Ru$_2$Os** with those of **1·Os$_3$** and **2·Os$_3$** (see, e.g., Figure 4), we have found (Table III) that *the quenching of the luminescence of the Ru-based components is accompanied by a parallel sensitization of the luminescence of the Os-based units*.[27] This shows unequivocally that the quenching occurs by an energy-transfer mechanism.

The observed electronic energy transfer can occur in principle, either from Ru-based to Os-based units which belong to the same **1·Ru$_2$Os**, or **2·Ru$_2$Os**, species (intramolecular intercomponent energy transfer) or between units which belong to distinct **1·Ru$_2$Os**, or **2·Ru$_2$Os**, species (*intermolecular* energy transfer). Under the experimental conditions used (1.0×10^{-5} M solution) intermolecular energy transfer can be ruled out. This is clearly demonstrated by the results obtained with the 2:1 **1·Ru$_3$**–**1·Os$_3$** and **2·Ru$_3$**–**2·Os$_3$** mixtures. The luminescence intensity of such mixtures is $^2/_3$ that of isoabsorptive **1·Ru$_3$** and **2·Ru$_3$** solutions (Table III), as expected because the light adsorbed (at the 461 nm isosbestic point of **1·Ru$_3$**, **1·Os$_3$**, **2·Ru$_3$**, and **2·Os$_3$**) by the Ru-based chromophoric units in the mixtures is $^2/_3$ that absorbed by the reference **1·Ru$_3$** and **2·Ru$_3$** solutions. Thus, the observed energy-transfer quenching/sensitization process must take place between Ru-based and Os-based components within each supramolecular species. Energy transfer from Ru(II) to Os(II) polypyridine complexes appended to a soluble polymer has also been recently observed by Meyer et al.[7f]

In the case of **2·Ru$_2$Os**, the residual Ru-based luminescence intensity is 50% that of the 2:1 **2·Ru$_3$**–**2·Os$_3$** mixture. The luminescence lifetime, however, is almost the same in the two cases. In the case of **1·Ru$_2$Os**, the Ru-based luminescence intensity reduces to 4%, and the luminescence lifetime is again almost unchanged. The behavior of **1·Ru$_2$Os** could be accounted for by assuming that energy transfer is very fast and 100% efficient and that the residual 4% luminescence intensity is due to the presence of small amounts of **1·Ru**, **1·Ru$_2$**, or **1·Ru$_3$** impurities,[28] although this is unlikely in view of the synthetic and purification procedures used. The behavior of **2·Ru$_2$Os**, where the residual luminescence intensity is 50%, cannot certainly be accounted for by the presence of impurities. Therefore we must conclude that in the **2·Ru$_2$Os** supramolecular species (and likely also in the **1·Ru$_2$Os** one) the quenching of the luminescence intensity is apparently not accompanied by a parallel quenching of the luminescence lifetime. This cannot be explained by a simple mechanism based on the occurrence of energy transfer in direct competition with the decay of the luminescent level in a single species. Mechanisms involving two (or more) excited states of the energy donor unit or two (or more) different geometrical conformations of the supramolecular structure must be invoked.

Energy transfer from a singlet MLCT level of the Ru-based components to a singlet MLCT level of the Os-based components in competition with ^{1}MLCT → ^{3}MLCT intersystem crossing in the Ru-based components could account for the observed results. This hypothesis, however, does not seem likely because deactivation of upper excited states to the lowest ^{3}MLCT level occurs in the picosecond time scale for $Ru(bpy)_3^{2+}$;[30] furthermore, there is no reason why energy transfer should not take place also from the ^{3}MLCT luminescent level.

In view of the flexibility of the supramolecular array, different spatial arrangements are likely to be present. The observed results are consistent with the presence of conformers in which energy transfer cannot occur, and conformers in which energy transfer takes place with a very fast rate. As schematized in Figure 9, two limiting geometrical arrangements can be considered, with

(26) Excited-state energies have been estimated as the energy of the emission maximum at 77 K. Other methods [refs 7a and 7e] give more refined but practically equivalent results.

(27) For the complex of **2** the experimental uncertainty is large because of the strong interference of the residual Ru-based emission.

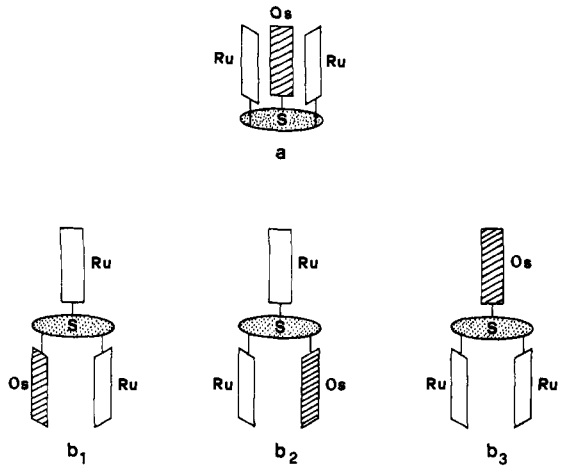

Figure 9. Possible conformers for the **1·Ru$_2$Os** and **2·Ru$_2$Os** supramolecular species. For more details, see text.

the three arms of the supramolecular species lying on the same side (a) or on different sides (b) with respect to the plane defined by the spacer. Since the excited-state lifetime of the luminescent Ru-based components is about 200 ns, the presence of different conformers will be relevant for energy transfer only if the rate of conformational interchange is slow on this time scale. This is indeed likely since inspection of molecular models shows that rotation around the C–C and C–N bonds which connect the bpy arms to the spacer is at least partially hindered because of the bulkiness of the three metal based components. Rotation around the N–CO bond, on the other hand, is known to be very slow because of the partial double bond character of the amide bond.[31]

Within the hypothesis of the presence of different conformers, an attempt to interpret the experimental results from a quantitative point of view can be performed. For type (b) arrangement, that should be more stable than type (a), the three situations depicted in Figure 9 are almost equivalent on energetic grounds. For similar complexes with only two arms NMR evidences for stacking of the aromatic rings contained in the spacer have been obtained.[32] In b_1 and b_2, one of the two Ru-based components is close to the Os-based component and energy transfer could thus take place at a very fast rate. The second Ru-based component, however, lies on the other side of the plane, so that its luminescence should not be affected.[33] This would also be the case for the two Ru-based components of conformer b_3. A statistical distribution among three conformers of type b (Figure 9) would leave 67% of residual luminescence intensity (as compared to the luminescence of the isoabsorptive 2:1 mixture of the parent homotrimetallic species). For **2·Ru$_2$Os**, however, the residual luminescence is about 50%. This result requires the presence of a fraction of conformers of type (a), where the three components are close to one another so that both the Ru-based luminescent components can be efficiently quenched by the Os-based component. The almost complete quenching of the Ru-based luminescence intensity for **1·Ru$_2$Os** can be accounted for by considering that the distance between the two Ru-based components and the Os-based component is short enough to ensure a fast through-space energy transfer practically in any geometrical conformation. A concomitant (or even predominant) occurrence of through-bond energy transfer, however, is likely in the case of **1·Ru$_2$Os** because of the smaller spacer.

The mechanism of energy transfer in similar complexes has been discussed in detail by Furue et al.[7b] and by Schmehl et al.[36] In view of the partial singlet character of the ^{3}MLCT level of the osmium–diimine complexes, a Förster-type (resonance) interaction[34] can play an important role.[7b] However the close approach of the donor and acceptor partners in the conformers where the quenching seems to take place (Figure 9) suggests that a through-space Dexter-type (exchange) interaction[35a] may be more likely in our systems.

An evaluation of the rate constant of the energy-transfer process in the **2·Ru$_2$Os** species which exhibit a conformation suitable for quenching can be obtained from eq 2, where $I°$ and $\tau°$ are the luminescence intensity and lifetime of the species that can be quenched, and I is their residual luminescence intensity after

$$k_{et} = 1/\tau°(I°/I - 1) \qquad (2)$$

quenching. The last quantity can be evaluated by comparing the total (from quenched and unquenched species) residual luminescence intensity (measured under stationary conditions by a fluorimeter) and the residual luminescence intensity $I(t)$ of the unquenched species (measured from laser experiment at $t > 100$ ns). For **2·Ru$_2$Os** these two experimental values are equal, (50 ± 2)%, within the experimental error. Therefore, the residual luminescence intensity of the quenched species is at most 2%. Using $I° = 50\%$, $I \leq 2\%$, and $\tau = 200$ ns, from eq 1 one obtains $k_{et} > 1 \times 10^8$ s^{-1}.

Luminescent Behavior of Mixed-Valence Compounds. We have seen above that the three metal-based components of each homometallic **1·Ru$_3$**, **2·Ru$_3$**, **1·Os$_3$**, and **2·Os$_3$** species are equivalent and their interaction is weak since their oxidation takes place at the same potential (Table IV). Addition of Ce(IV) is therefore expected to lead to a statistical mixture of species where the three metal ions have +2 or +3 oxidation number. The four species involved can be indicated by II-II-II, II-II-III, II-III-III, and III-III-III, where the Roman numerals show the oxidation number of the three metal ions contained in the supramolecular species. The distribution of the four species for various amounts of added oxidant is shown in Figure 10.[37] As far as absorption is concerned, Ru(bpy)$_3^{2+}$, **1·Ru$_3$**, **2·Ru$_3$**, Os(bpy)$_3^{2+}$, **1·Os$_3$**, and **2·Os$_3$** behave in the same way (see, e.g., Figure 6): each equivalent of added oxidant transforms an equivalent of strongly absorbing (at 450 nm) metal(II)-based unit into a weakly absorbing metal(III)-based unit.[22] The luminescence behavior, however, is different. For Ru(bpy)$_3^{2+}$ and Os(bpy)$_3^{2+}$ a linear plot is again obtained (Figures 7 and 8) because each equivalent of added oxidant transforms a luminescent metal(II)-based unit into a nonluminescent metal(III)-based unit, and no intermolecular interaction can take place under the experimental condition used. For the supramolecular species, however, the experimental points lie *below* the straight line a (Figures 7 and 8) that represents the behavior of the separated M(bpy)$_3^{2+}$ units, indicating that there is a quenching effect of the metal(III)-based components on the

(28) We are well aware of the difficulties encountered to eliminate traces of luminescent impurities in dealing with polynuclear diimine-based Ru and Os complexes. This problem has also been encountered by many other research groups (see, e.g., refs 7a, 7b, and 29).

(29) Schanze, K. S.; Neyhart, G. A.; Meyer, T. J. *J. Phys. Chem.* **1986**, *90*, 2182.

(30) (a) Bradley, P. C.; Kress, N.; Hornberger, B. A.; Dallinger, R. F.; Woodruff, W. H. *J. Am. Chem. Soc.* **1989**, *103*, 7441. (b) Carrol, P. J.; Brus, L. E. *J. Am. Chem. Soc.* **1987**, *109*, 7613. (c) Yabe, T.; Anderson, D. R.; Orman, L. K.; Chang, Y. J.; Hopkins, J. B. *J. Phys. Chem.* **1989**, *93*, 2302. (d) Cooley, L. F.; Bergquist, P.; Kelley, D. F. *J. Am. Chem. Soc.* **1990**, *112*, 2612.

(31) Buhleier, E.; Wehner, W.; Vögtle, F. *Chem. Ber.* **1979**, *112*, 546, 559.

(32) Belser, P., work in progress.

(33) CPK model shows that for a fully extended **2·Ru$_2$Os** conformer the metal-to-metal distance is around 27 Å. An estimation of the energy-transfer rate constant over such a long distance by a Förster-type mechanism[34] gives a value of $\sim 1 \times 10^6$ s^{-1}, which is much smaller than the excited-state decay. On the other hand, a through bond[35] exchange energy transfer over the 24 bonds that separate the two metals seems unlikely.

(34) Förster, Th. H. *Discuss. Faraday Soc.* **1959**, *27*, 7.

(35) (a) Dexter, D. L. *J. Chem. Phys.* **1953**, *21*, 836. (b) Oliver, A. M.; Craig, D. C.; Paddon-Row, M. M.; Kroon, J.; Verhoeven, J. W. *Chem. Phys. Lett.* **1988**, *150*, 366. (c) Hoffman, R.; Imamura, A.; Here, W. J. *J. Am. Chem. Soc.* **1968**, *90*, 1499.

(36) Schmehl, R. H.; Auerbach, R. A.; Walcholtz, W. F. *J. Phys. Chem.* **1988**, *92*, 6202.

(37) The fractions of the four species are given by $(1-x)^3$, $3\cdot(1-x)^2\cdot x$, $3\cdot(1-x)\cdot x^2$, and x^3, where x is fraction of added oxidation equivalents.

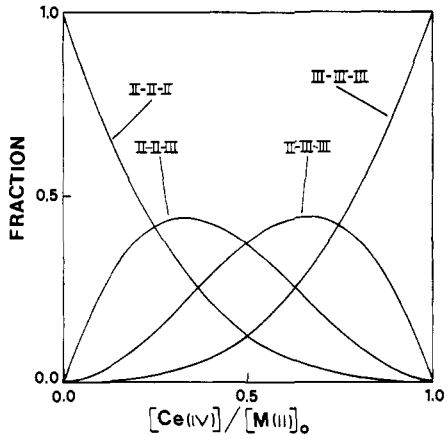

Figure 10. Statistical distribution of the four species which are present in solutions of partially oxidized trinuclear Ru(II) and Os(II) complexes.

luminescent metal(II)-based ones. Since the concentration of the solution is very low, encounters between separated species cannot occur during the excited-state lifetime as is also shown by the "regular" behavior of the separated $M(bpy)_3^{2+}$ units. Therefore, the observed quenching must occur within each supramolecular species (*intercomponent* quenching). Under such conditions, the fraction of luminescence intensity can never be less than that generated by the fraction of II-II-II species that are present in the solution, since their metal(II)-based units cannot be quenched. Such a lower limiting value for the luminescence intensity on increasing the amount of added oxidation is represented by curve b in Figures 7 and 8. As one can see, the experimental values for **1·Ru$_3$** and **1·Os$_3$** lie on such a curve. This shows that in the II-II-III and II-III-III mixed-valence forms of the **1·Ru$_3$** and **1·Os$_3$** supramolecular species the luminescence of the M(II)-based units is totally quenched. These results parallel that found for the energy-transfer process in the **1·Ru$_2$Os** species, where the Os-based component quenches almost completely the Ru-based luminescent units. For the **2·Ru$_3$** and **2·Os$_3$** species, the values of the luminescent intensity on addition of Ce(IV) lie between curve a and b of Figures 7 and 8, respectively, indicating that the II-II-III and/or (less likely) II-III-III species are partially luminescent. This can be accounted for by the presence of conformers where quenching can occur and conformers where quenching cannot occur, as discussed in the previous section for energy transfer in the **2·Ru$_2$Os** species (Figure 9). Since the experimental points are rather scattered (Figures 7 and 8), we prefer to avoid speculations about the fractions of luminescent conformers in the mixed-valence species. It should also be recalled that the solvent used for the Ru and Os species are different (see Experimental Section).

The quenching of the luminescent excited state of the M(II) components by the M(III) components in the mixed-valence species can take place, in principle, by energy or electron transfer. Figure 11 schematizes the competition between the "intracomponent" decay of the luminescent ^{3}MLCT excited state of a M(II) unit (k_d), and the decay via (i) energy transfer to the ^{3}LMCT excited state of the M(III) unit (k_{en}) which then relaxes to the ground state (k'_d), and (ii) electron transfer to a M(III) component (k_{el}) which yields the intervalence transfer "isomer" of the ground state. Our results show that $k_{el} + k_{en} \gg k_d$ for the compounds of **1** and $k_{el} + k_{en} \simeq k_d$ for the compounds of **2**. This contrasts with the behavior observed by Meyer et al.[7d] in soluble polymers with appended Os(II) and Os(III) polypyridine complexes, where no quenching was observed.

As we have seen above, the excited-state energy is 2.08 eV for the Ru(II) units and 1.72 eV for the Os(II) units. For the Ru(III) units, the lowest excited state, which is ligand-to-metal CT in nature, lies around 1.83 eV, so that energy transfer (k_{en}, Figure 11) is thermodynamically favored. The lowest excited state of the Os(III) unit, which is again LMCT in nature, lies at 2.2 eV.[38] As a consequence, the energy-transfer process in the case of **1·Os$_3$** and **2·Os$_3$** is thermodynamicially unfavorable (Figure 11) and can thus be ruled out as a quenching mechanism. Our results show that the quenching is almost equally efficient in the Ru-based and Os-based supramolecular species (Figures 7 and 8). This suggests that energy transfer is not involved even in the case of the Ru complexes.[39] The competition for the decay of the luminescent excited state in **1·Os$_3$**, **2·Os$_3$**, and perhaps also in **1·Ru$_3$** and **2·Ru$_3$** seems therefore restricted to the processes of rate constants k_d and k_{el} (Figure 11). Such processes can be viewed as electron-transfer processes or as radiationless decay processes occurring between states of a supramolecular species.[41] For **1·Ru$_3$** and **1·Os$_3$**, the electronic interaction between the bpy ligands of the M(II) and M(III) components is likely to be large enough to put the electron-transfer process of rate constant k_{el} in the adiabatic regime. This, of course, is certainly the case for the process of rate constant k_d. Both processes have the same, very large and negative, free energy change (−2.08 eV for the Ru species; −1.72 eV for the Os species). They must thus lie in the "inverted" region.[5,42-44] The faster process will therefore be that which exhibits the larger reorganizational energy. Looking at the scheme of Figure 11 and considering the electronic rearrangements caused by the two processes, it is easy to understand that the intercomponent electron-transfer process involves a change in the electric charge of the two units and thus requires an extensive solvent repolarization, whereas this is not the case for the other process. The intercomponent electron-transfer process will thus be faster than the intracomponent deactivation, which accounts for the observed luminescence quenching.

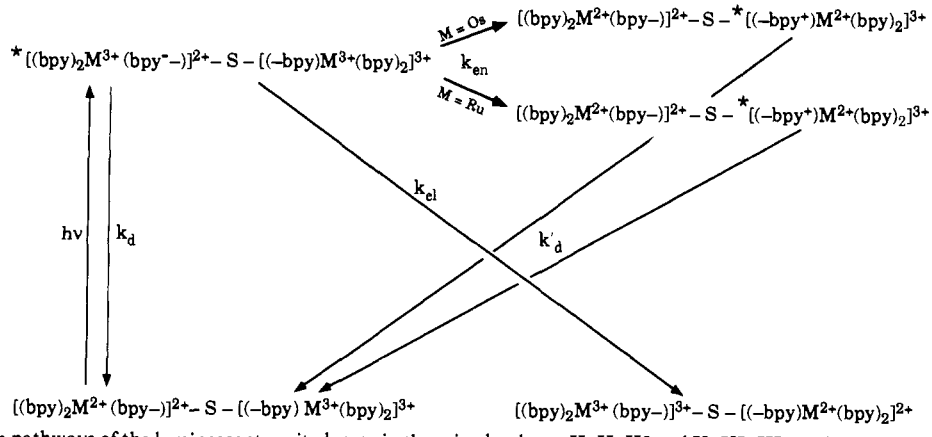

Figure 11. Deactivation pathways of the luminescent excited state in the mixed-valence II–II–III and II–III–III species, exemplified on a II–III species for the sake of simplicity. For the S spacer, see **1** or **2** in Figure 1.

For the **2·Ru$_3$** and **2·Os$_3$** species, the electronic interaction for the intercomponent electron-transfer process is smaller (because of the larger spacer) than in the case of the species involving **1**. This could be the reason why k_{el} is comparable to (instead of much larger than) k_d for these species.

Finally, we would like to compare briefly the behavior of our systems with that found for soluble styrene/chloromethylstyrene polymers containing about 30 appended Ru(II) and/or Os(II) polypyridyl complexes.[7d] In the extended (energy minimized) structure the separation distance between two components in the polymer is 21 Å,[7f] i.e., almost the same as that found in the extended structure of the compounds of **2**. Both in the polymeric Ru(II)–Os(II) species[7f] and in **2·Ru$_2$Os** energy transfer takes place. The mixed-valence Ru-based polymers compound could not be studied because of the intrinsic instability of the polymer when linked to Ru(III).[7f] For the mixed-valence Os-based polymer compound, no quenching of the excited Os(II) sites by the Os(III) sites was observed,[7f] contrary to what happens for the mixed-valence Os-based compounds of **2**. A possible explanation for this different behavior could be a lower reorganizational barrier (due to a different "solvation" environment) which leaves the electron-transfer quenching process for the polymer in a deeper Marcus inverted region. This effect could arise not only because of different solvents used (CH_3CN for the polymer system,[7d] CH_3CN/H_2O 5:1 v/v for **2·Os$_3$**) but also because of a different local environment provided by the different supramolecular structures.

Acknowledgment. We would like to thank Dr. A. Schäfer (Institut für Organische Chemie, University of Zürich) for the electrospray ionization measurements and for some FAB data. We would also like to thank L. Minghetti for technical assistance and G. Gubellini for the drawings. This work was supported by MURST and CNR (Italy), Swiss National Science Foundation (Switzerland), and "Bundesministerium fur Forschung und Technologie", Project No. 0329120 A (Germany).

(38) Os(III) is a worse oxidant than Ru(III); therefore the LMCT transitions lie at higher energy in the Os(III) compound. The values of 1.83 and 2.2 eV are those corresponding to the maximum of the lowest energy absorption band.[22] The zero–zero transition is expected to be 0.2–0.3 eV lower in energy.

(39) Considerations based on localized molecular orbital configurations show that energy transfer by an exchange mechanism would imply the simultaneous transfer of two electrons (Figure 11):[40] one from the bpy ligand of a M(II) unit to the metal of a M(III) unit and the other from the bpy ligand of a M(III) unit to the metal of a M(II) unit. Both the intracomponent deactivation (k_d) and intercomponent electron transfer (k_{el}), by contrast, imply a one-electron transfer: from the bpy ligand to its coordinated metal in the former case and from the bpy ligand of a M(II) component to the bpy ligand of a M(III) component in the latter.

(40) In more appropriate terms, one should speak about a simultaneous overlap of the corresponding wave functions.

(41) In general there is a close relationship between excited-state decay and elementary electron-transfer reactions. The rates of both types of processes are controlled by the Franck–Condon or vibrational overlap factors which have their origins in the differences in molecular structure and solvation between the reactants and products.[42]

(42) (a) Kestner, N. R.; Logan, J.; Jortner, J. *J. Phys. Chem.* **1974**, *78*, 2148. (b) Efrina, S.; Bixon, M. *Chem. Phys.* **1976**, *13*, 447. (c) Balzani, V.; Bolletta, F.; Scandola, F. *J. Am. Chem. Soc.* **1980**, *102*, 2152. (d) Orlandi, G.; Monti, S.; Barigelletti, F.; Balzani, V. *Chem. Phys.* **1980**, *52*, 313. (e) Scandola, F.; Balzani, V. *J. Chem. Educ.* **1983**, *60*, 816. (f) Kober, E. M.; Caspar, J. V.; Lumpkin, R. S.; Meyer, T. J. *J. Phys. Chem.* **1986**, *90*, 3722. (g) Sigman, M. E.; Closs, G. L. *J. Phys. Chem.* **1991**, *95*, 5012.

(43) Marcus, R. A. *Discuss. Faraday Soc.* **1960**, *29*, 21.

(44) Marcus, R. A.; Sutin, N. *Biochim. Biophys. Acta* **1985**, *811*, 265.